Current Research in Toxicology 7 (2024) 100192

Contents lists available at ScienceDirect

Current Research in Toxicology

journal homepage: www.journals.elsevier.com/current-research-in-toxicology

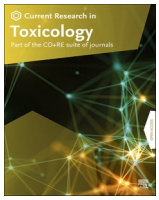

Environmental cadmium-induced circRNA-miRNA-mRNA network regulatory mechanism in human normal liver cell model

Zhi Qu [a,b,1], Lugang Deng [a,c,1], Chunqian Feng [d], Peisen Guo [e], Peixi Wang [b], Nan Liu [a,b,*]

[a] Institute of Environment and Health, South China Hospital of Shenzhen University, Shenzhen 518116, China
[b] School of Nursing and Health, Henan University, Kaifeng 475004, China
[c] School of Public Health, Guangzhou Medical University, Guangzhou 511436, China
[d] School of Medicine, Shangqiu Institute of Technology, Shangqiu 476000, China
[e] The Center of Gastrointestinal and Minimally Invasive Surgery, Department of General Surgery, The Third People's Hospital of Chengdu, The Affiliated Hospital of Southwest Jiaotong University, Chengdu 610031, China

ARTICLE INFO

Keywords:
Cadmium
CeRNA
CircRNA
Environmental factor
L-02 cell

ABSTRACT

At present, hundreds of long non-coding RNAs (lncRNAs) and microRNAs (miRNAs) have been confirmed to be related to the toxicity of cadmium (Cd). However, the role of circular RNAs (circRNAs) in the toxicity of Cd and the underlying regulatory mechanisms remain unclear. In this study, we chose human normal liver cells (L-02) as a model to investigate changes in transcriptome expression levels following exposure to Cd. Total RNA of each sample was extracted by Trizol method, and the expression profiles of circRNAs, miRNAs and mRNAs of each sample were determined by microarray hybridization and scanning. After standardizing the data, differential circRNAs, miRNAs, and mRNAs associated with the toxic effects of Cd were identified. By screening the predicted circRNAs, miRNAs, and mRNAs, we constructed a competing endogenous RNA (ceRNA) network, and predicted the main biological functions and metabolic pathways influenced by Cd toxicity. Our comprehensive screening strategy led to the identification of 266 different circRNAs, 223 different miRNAs and 519 different mRNAs exhibiting differential expression. Following further screening, even circRNAs, 10 miRNAs and 97 mRNAs were incorporated into the ceRNA network. After performing GO enrichment and KEGG pathway analyses on the 97 mRNAs within the ceRNA network, which indicated that the circRNAs in the ceRNA network are poised to modulate key cellular processes, including cell proliferation, apoptosis, oxidative stress and inflammatory responses under the toxic effects of Cd-induced damage in L-02 cells.

Introduction

Cadmium (Cd), a persistent and non-essential heavy metal element, widely exists in various industrial commodities, and is a representative environmental heavy metal contaminant. Exposure to environmental Cd poses significant health risks to humans, primarily through contamination of the food chain and drinking water sources (Bernhoft, 2013). This results in acute and chronic damage to vital organs, including the kidney, liver, bone, and reproductive system (Johri et al., 2010; Wang et al., 2021a). Cd infiltrates organisms via environmental exchange and accumulates progressively due to its lengthy half-life, with potential carcinogenic outcomes. A substantial number of epidemiological investigations showed that the damage of Cd to human target organs was manifested as disorders related to calcium and phosphorus metabolism. Bone-related pathologies such as osteoporosis, osteoarthritis, and osteomalacia are direct consequences (Ma et al., 2021). Furthermore, dysfunction of the male and female reproductive system and disturbances in hormone synthesis and regulation, have been observed in several studies. It is noteworthy that even at low doses, Cd can diminish fertility rates and contribute to untoward outcomes during pregnancy (Kumar and Sharma, 2019). In addition, Cd disrupts the intraorganismal equilibrium and metabolism of essential trace elements *in vivo* (Zhou et al., 2015). Cd exposure triggers oxidative stress, destabilizes the mitochondrial membrane potential, provokes injuries to DNA molecular and hampers the DNA repair mechanism (Bertin and Averbeck, 2006).

As the main Cd storage and metabolism organ, liver is the most sensitive organ to Cd toxicity. Numerous studies have demonstrated that Cd induces liver toxicity through the mechanisms involving apoptosis

* Corresponding author.
E-mail address: 13688869875@163.com (N. Liu).
[1] Both authors contributed equally to this paper.

https://doi.org/10.1016/j.crtox.2024.100192
Received 3 June 2024; Received in revised form 27 July 2024; Accepted 23 August 2024
Available online 24 August 2024

and inflammatory stimulation. Zoology experiments showed that the serum levels of aspartic acid transaminase (AST), alanine aminotransferase (ALT), alkaline phosphatase (ALP) and lactate dehydrogenase (LDH) in rats were abnormally elevated. Liver biopsy indicates congestion, infiltration, alterations in hepatocyte lumen, and edema, indicative of inflammation and liver damage (Sanjeev et al., 2019).

Circular RNAs (circRNAs) constitute a significant class of non-coding RNA (ncRNA), purposefully produced through back-splicing of free 3′ and 5′ ends. Abundant evidence suggests that circRNAs are widespread in various species and cell lines (Chen and Yang, 2015). Advances in high-throughput sequencing technology has significantly facilitated our comprehension of circRNAs' regulatory functions. Primarily, circRNAs serve as sponges for microRNAs (miRNAs), regulating their activity and consequently influencing the expression of targeted messenger RNAs (mRNAs) (Panda, 2018). Secondly, they directly bind to specific proteins, regulating gene transcription through interactions, and influenceing cellular processes such as proliferation, cell cycle progression and apoptosis (Du et al., 2016). Additionally, certain circRNAs contain internal ribosomal entry sites that have the capability to directly encode proteins (Pamudurti et al., 2017). Despite growing interest in circRNAs, studies linking them to the toxicity of Cd are scarce. Wang et al. investigated human bronchial epithelial cells as a model for chronic Cd exposure, revealing a significant down-regulation of circSPAG16 in chronically exposed cells through high-throughput sequencing (Wang et al., 2021b). A separate study demonstrated that hsa_circ_0040768 is involved in the protective effect of Caffeic acid phenethyl ester against Cd-induced autophagy by targeting MAP1LC3B. These findings provide novel insights into the pathogenesis, as well as potential prevention and treatment of Cd-related diseases (Hao et al., 2020).

Transcriptome investigations have primarily focused on the effects of Cd on long noncoding RNAs (lncRNAs), miRNAs and mRNAs. Nevertheless, the exploration of the regulatory mechanisms governing the circRNA network in Cd-induced cellular damage has received scant attention. The repercussions of Cd-induced toxicity on circRNA function and its associated regulatory pathways remain largely uncharted territory. In this study, human normal liver cells (L-02) were selected as the experimental model to investigate variations in the comprehensive transcriptome expression profiles in response to Cd toxicity. In addition, enrichment analysis was utilized to determine the impact of Cd exposure on cellular components, molecular functions, biological processes and metabolic pathways.

Furthermore, we have established the competitive endogenous RNA (ceRNA) regulation networks for the first time, thereby facilitating insights into the regulatory mechanism of circRNA-miRNA-mRNA interactions and their primary biological functions following Cd exposure. Our investigation has identified novel circRNA biomarkers associated with Cd exposure and has elucidated the ceRNA regulatory paradigm involving circRNAs. This provides a scientific foundation for understanding the ecological safety implications of Cd exposure and offers inspiration for further exploration of the relationship between Cd and circRNAs.

Materials and methods

Cell culture and reagents

Human normal liver L-02 cell line (No. HL-7702) was obtained from Fuheng Biology Ltd. (Shanghai, China) and underwent authentication through short tandem repeat (STR) profiling, resulting in good genetic typing and with no vidence of multiple alleles. Mycoplasma testing confirmed the absence of contamination, and microscopic examination revealed no bacterial or fungal contaminants. The cells were cultured in complete medium containing 10 % fetal bovine serum (Gibco, Catalog No. 10099-141) under standard conditions of 37℃ and 5 % CO_2.

Cd exposure and analysis

L-02 cells in logarithmic growth phase were divided into two sets of experimental groups: one set treated with $CdCl_2$ at concentrations of 10, 20, 30, 40, 50 and 60 μM for 12, 24, 48 and 72 h, and a control group. The cell viability within each group was determined by CCK-8 assay. Measurement of absorbance at 450 nm was performed on a microplate reader (Multiskan GO, Thermo-Fisher Scientific, Waltham, MA, USA) for each individual well to ascertain the respective cellular tendencies. To explore the differential expression of circRNAs, miRNAs, and mRNAs, L-02 cells were exposed to 20 μM $CdCl_2$ for 72 h as the treatment group for subsequent whole-transcriptome microarray analysis. For the control group, L-02 cells were cultured under standard conditions for the equivalent duration.

RNA extraction, quantification and identification

Total RNA, including circRNA, miRNA and mRNA, was extracted from each sample using the TRIzol reagent method. Subsequent RNA purification was performed using the RNasey Mini Kit (Qiagen p/n 74104, USA). The concentration of the total RNA from each sample was quantified by NanoDrop® ND-1000 (Thermo-Fisher Scientific, USA). The integrity of the RNA samples and the presence of genomic DNA (gDNA) contamination were assessed through agarose gel electrophoresis.

Hybridization and scanning of the microarrays

After labeling, the circRNA, miRNA and mRNA from each sample were hybridized onto their respective microarrays-Arraystar Human circRNA Array V2 (8 × 15 K, Arraystar Inc., USA), Agilent Human miRNA Microarray, Release 21.0 (8 × 60 K, Agilent Inc., USA) and Agilent Human Gene Expression Microarrays V2 (4 × 44 K, Agilent Inc., USA) following the manufacturer's protocols. Following thorough cleaning and washing, the microarrays were scanned utilizing an Agilent Scanner G2505C (Agilent Technologies, USA). Subsequent image analysis and data processing to derive the raw data were executed using Agilent Feature Extraction Software, version 12.0.

(1) circRNA: The extracted and purified total RNA from each sample underwent treatment with Rnase R enzyme aimed at eliminating linear RNA and enriching circRNA. Following random primer method (Arraystar Super RNA Labeling Kit; Arraystar, USA) for amplification and transcription, the enriched circRNAs were converted into fluorescent cRNAs. Subsequently, the labeled cRNA was hybridized with Arraystar Human circRNA Array V2 (8 × 15 K, Arraystar Inc., USA) microarray and incubated for 17 h at a temperature of 65℃ within an Agilent hybridization furnace. After cleaning and washing, the microarrays were scanned with an Agilent Scanner G2505C Microarray Scanner (Agilent Technologies, USA). Analysis of the microarray images and data processing to obtain the original data was performed using Agilent Feature Extraction software 12.0.
(2) miRNA: MiRNA from each sample was labeled with Cyanine 3-PCP using T4 RNA LIGase. Subsequently, the labeled products were concentrated, dried, and re-dissolved in water. Hybridization with Agilent Human miRNA Microarray, Release 21.0 (8 × 60 K, Agilent Inc., USA) microarray was then utilized for hybridization at 55℃ for 20 h. After washing of the hybrid microarray, the same procedure as described earlier was performed.
(3) mRNA: Total RNA of each sample was linearly amplified with CY3-UTP Labeling by Quick Amp Labeling Kit, One-color (Agilent P/N 5190-0442, USA). The labeled cRNAs were then purified using the RNeasy Mini Kit (Qiagen, USA), and their concentration and activity were verified by employing of NanoDrop ND-1000. Hybridization with Agilent Human Gene Expression

Microarrays V2 (4 × 44 K, Agilent Inc., USA) microarray was performed at a temperature of 65℃ for 17 h. After washing the hybrid microarray, the same aforementioned steps were undertaken.

Screening and clustering analysis of differentially expressed RNAs

The comprehensive expression profiles were analyzed to identify differentially expressed circRNAs, miRNAs, and mRNAs between the control and Cd-exposed groups. To visualize these differentially expressed RNAs, R software was employed to generate Volcano and Clustering heatmaps, respectively.

Gene Ontology (GO) and kyoto encyclopedia of genes and genomes (KEGG) pathway analysis

To elucidate the functional implications of the differentially expressed mRNAs, we conducted GO enrichment analysis and KEGG metabolic pathway analysis. The GO analysis includes cellular component (CC), molecular function (MF) and biological process (BP) which provide insights into the biological functions of the differentially expressed genes. A stringent screening criterion of $P<0.05$ was applied to identify significantly enriched GO terms, with decreasing P values indicative of increasingly substantial enrichment of genes within the corresponding category. Similarly, KEGG metabolic pathway analysis reveals the biological metabolic pathways associated with the differential genes. A lower P value denoted a greater degree of enrichment of these genes in the associated pathway.

Construction of the circRNA-miRNA-mRNA network

CircRNAs are known to contain numerous miRNA response elements (MREs), enabling them to act as miRNA sponges for multiple miRNAs. To pinpoint the potential target miRNAs of circRNAs, we capitalized on the Target Scan prediction tool within the CircInteractome database (https://circinteractome.irp.nia.nih.gov/). Specifically, we cross-referenced the predicted miRNAs against those found to be differentially expressed, retaining the intersecting set for subsequent analysis. These miRNAs exert their regulatory effects on specifically targeted mRNAs through sequence complementarity, leading to mRNA degradation or inhibition of protein translation. To identify the prospective targets of these miRNAs, we employed miRWalk 3.0 database, and the predicted mRNAs were subsequently intersected with those exhibiting differential expression for further analysis. Based on the standardized expression profiles of circRNAs, miRNAs, and mRNAs within the aforementioned network, Pearson correlation analysis was performed to identify mRNAs co-expressed with circRNAs and miRNAs negatively correlated with the expression levels of both circRNAs and mRNAs. The criterion for screening was a significance level of $P<0.05$. The resultant ceRNA interactions obtained from the analytical screening, were visualized as a network using Cytoscape 3.8.1.

Real-time fluorescence quantitative PCR (RT-qPCR) for circRNA analysis

To validate the reliability of the RNA glass slide hybridization, the expression levels of the target circRNAs were quantified via RT-qPCR. The samples were placed in a fluorescent quantitative PCR instrument (CFX96, Bio-Rad Laboratories, Inc.), following the operating instructions of GoScript™ Reverse Transcription System (A5001, Promega, USA) kit. Quantitative amplification was conducted, and the resulting melting curves were analyzed. The expression of each gene was calculated using the relative quantification method ($2^{-\Delta\Delta Ct}$), based on the selection of specific and efficient amplification products.

Statistical analysis

All experiments were conducted in triplicate to ensure consistency and reliability. The data were statistically analyzed using Origin 2022 (OriginLab Co., Northampton, MA, USA) and SPSS software 26.0 (SPSS Inc., Chicago, IL, USA). Comparative analysis between two groups was carried out using the Student's *t*-test, whereas comparisons across three or more groups were addressed with a one-way ANOVA. For comparing variances between two groups, either Dunnett's T method or Dunnett's T3 method was applied ($\alpha = 0.05$, $P<0.05$). Subsequently, GO analysis, KEGG analysis and Pearson correlation analysis were carried out using R software.

Results

The effect of $CdCl_2$ on the activity of L-02 cells after exposure

In our study, when exposure to the $CdCl_2$ with low-concentration, "Hormesis" effect could be observed for 12 h. The survival rate of L-02 cells, serving as a proxy for cellular health, became significantly lower, reflecting a direct and negative correlation between exposure time and concentration, with statistical significance ($P<0.05$) (Fig. 1).

Following a 12 h exposure to $CdCl_2$ on L-02 cells for 12 h, we observed an increase in cell proliferation in 10 and 20 μM groups. However, the survival rates in 50 and 60 μM groups were significantly decreased by 24 % and 37 % ($P<0.05$), respectively. As the duration of exposure to 24, 48 and 72 h, the cell survival rate in each concentration group progressively decreased. The 30 and 40 μM groups exhibited inhibitory effect on cell growth at 24 h, leading to a decrease in the cell survival rate by 30 % and 53 % ($P<0.05$), respectively. Notably, the 20 μM group, which initially showed a hormetic response, demonstrated a significant inhibitory effect ($P<0.05$) at 72 h, with a 15 % decrease in cell survival rate. These findings offer initial insights into the proliferative toxicity of $CdCl_2$ on L-02 cells, highlighting both potential stimulation at lower concentrations and toxicity at higher concentrations over time.

Differential expression of circRNAs, miRNAs and mRNAs

The differential expression analysis unveiled a comprehensive landscape of RNA regulation, identifying 266 differentially expressed circRNAs with 134 up-regulated and 132 down-regulated, 223 differentially expressed miRNAs including 65 up-regulated and 158 down-regulated, 519 differentially expressed mRNAs consisting of 365 up-regulated and 154 down-regulated (Fig. 2).

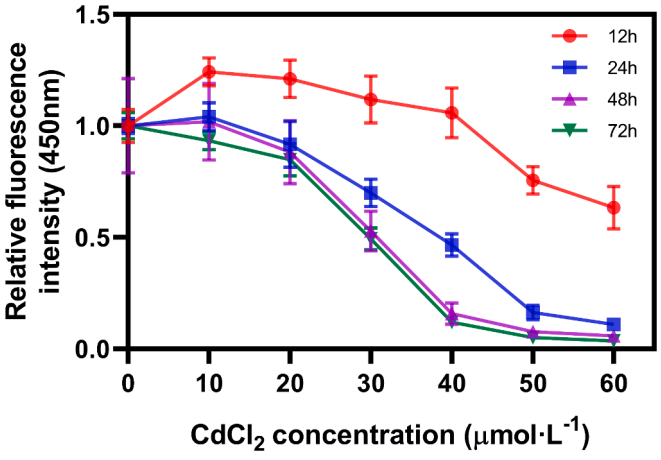

Fig. 1. The relative fluorescence intensity when L-02 cell exposing to $CdCl_2$ at different concentrations and time points.

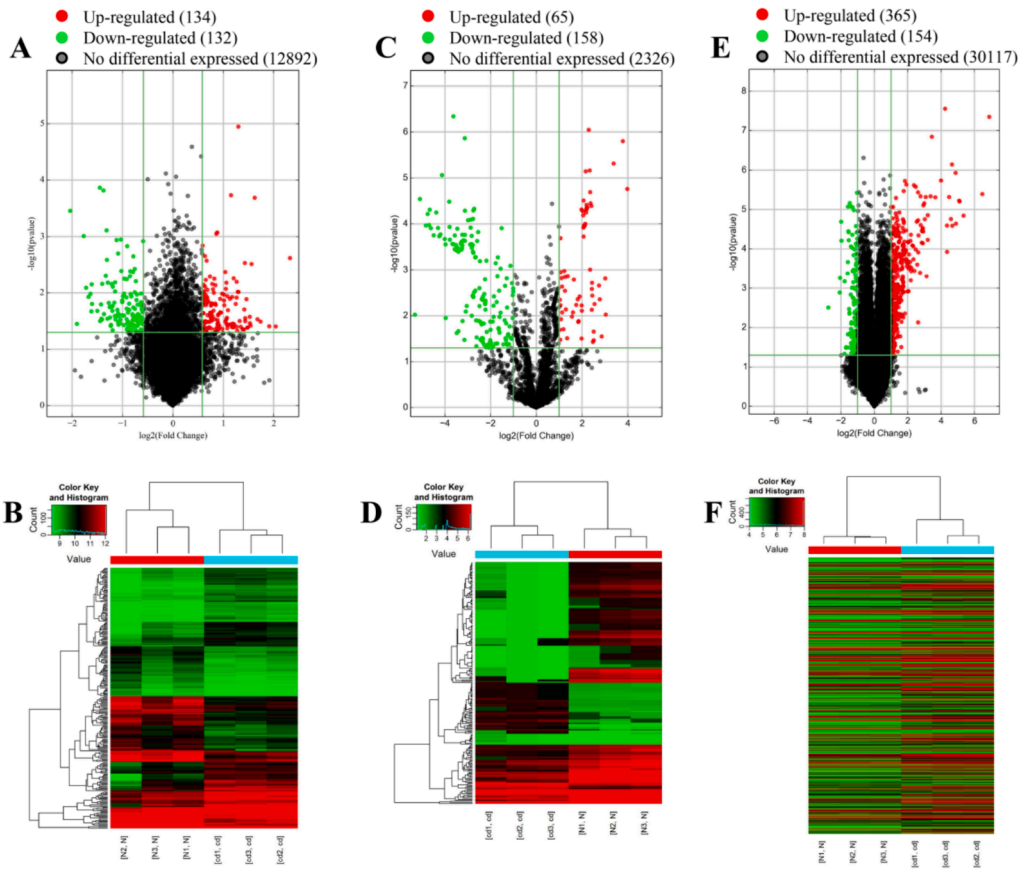

Fig. 2. Differentially expressed volcano map and cluster heatmap. (A) circRNA differentially expressed volcano map; (B) circRNA cluster heatmap; (C) miRNA differentially expressed volcano map; (D) miRNA cluster heatmap; (E) mRNA differentially expressed volcano map; (F) mRNA cluster heatmap.

GO enrichment analysis and KEGG pathway analysis of differentially expressed mRNAs

Following GO enrichment and KEGG pathway analysis of the 365 up-regulated mRNAs, a total of 44 cellular components terms, 59 molecular function terms, 859 biological processes terms, and 51 biological pathways were significantly enriched ($P<0.05$). Similarly, for the 154 down-regulated mRNAs, the analysis revealed 24 cellular component terms, 42 molecular function terms, 239 biological process terms and 2 biological pathways that were significantly enriched ($P<0.05$) (Fig. 3).

Construction of circRNA-miRNA-mRNA regulatory network

Using stringent bioinformatics criteria, we constructed a ceRNA network focusing on circRNAs that showed either the top 10 fold changes or the top 10 most significant *P* values. The circRNA-miRNA-mRNA pairs were identified through bioinformatics prediction from the CircInteractome database and miRWalk 3.0 database. A total of 9 differential circRNAs were identified, with 8 circRNAs showing significant up-regulation and one circRNA displaying significant down-regulation. Additionally, 12 differential miRNAs were retained, with 11 showing significant down-regulation and one displaying significant up-regulation. Furthermore, we identified 127 differential mRNAs, with 115 significantly up-regulated and 12 significantly down-regulated. Based on the preliminary predicted ceRNA pairs, we performed Pearson correlation tests with standardized expression data. It is noteworthy that the Person correlation test did not reveal any significant related miRNAs for hsa_circ_0092283 and hsa_circ_0092319. Ultimately, we constructed a comprehensive ceRNA network comprising of seven circRNAs (hsa_circ_0004662, hsa_circ_0000745, hsa_circ_0082546, hsa_circ_0082547, hsa_circ_0033388, hsa_circ_0002082 and hsa_circ_0017037), 10 miRNAs and 97 mRNAs (Fig. 4).

Go enrichment analysis and KEGG pathway analysis of mRNAs in ceRNA network

Upon conducting GO enrichment and KEGG pathway analysis on the 97 mRNAs within the circRNA-miRNA-mRNA network, we observed significant enrichment ($P<0.05$) across seven cellular components items, six molecular function items, 27 biological process items and five metabolic pathways. The significantly enriched terms included the positive regulation of apoptosis, inflammation, negative regulation of cell proliferation, negative regulation of interleukin-6 (IL-6) production, and cell–cell signaling, alongside pathways such as cytokine-cytokine receptor interaction, FoxO signaling, and NOD-like receptor signaling. These findings imply that circRNAs within the ceRNA network might potentially regulate cell proliferation, apoptosis, oxidative stress and inflammatory response in the presence of Cd-induced toxicity (Tables 1 and 2).

Verification of circRNA expression and circular structure

In ceRNA network, hsa_circ_0004662 and hsa_circ_0000745 are the two circRNAs exhibiting the greatest fold change in expression levels in conjunction with the aforementioned differential expression analysis. The expression levels of both hsa_circ_0000745 and hsa_circ_0004662 increased with the extend of exposure time, and the expression levels of hsa_circ_0004662 were up-regulated with the increase of exposure concentration, demonstrating statistical significance ($P<0.05$). Sanger sequencing confirmed that the unique back-splicing junctions of the two circRNAs were consistent with the sequences from the SOD2 and SPECC1, respectively (Fig. 5).

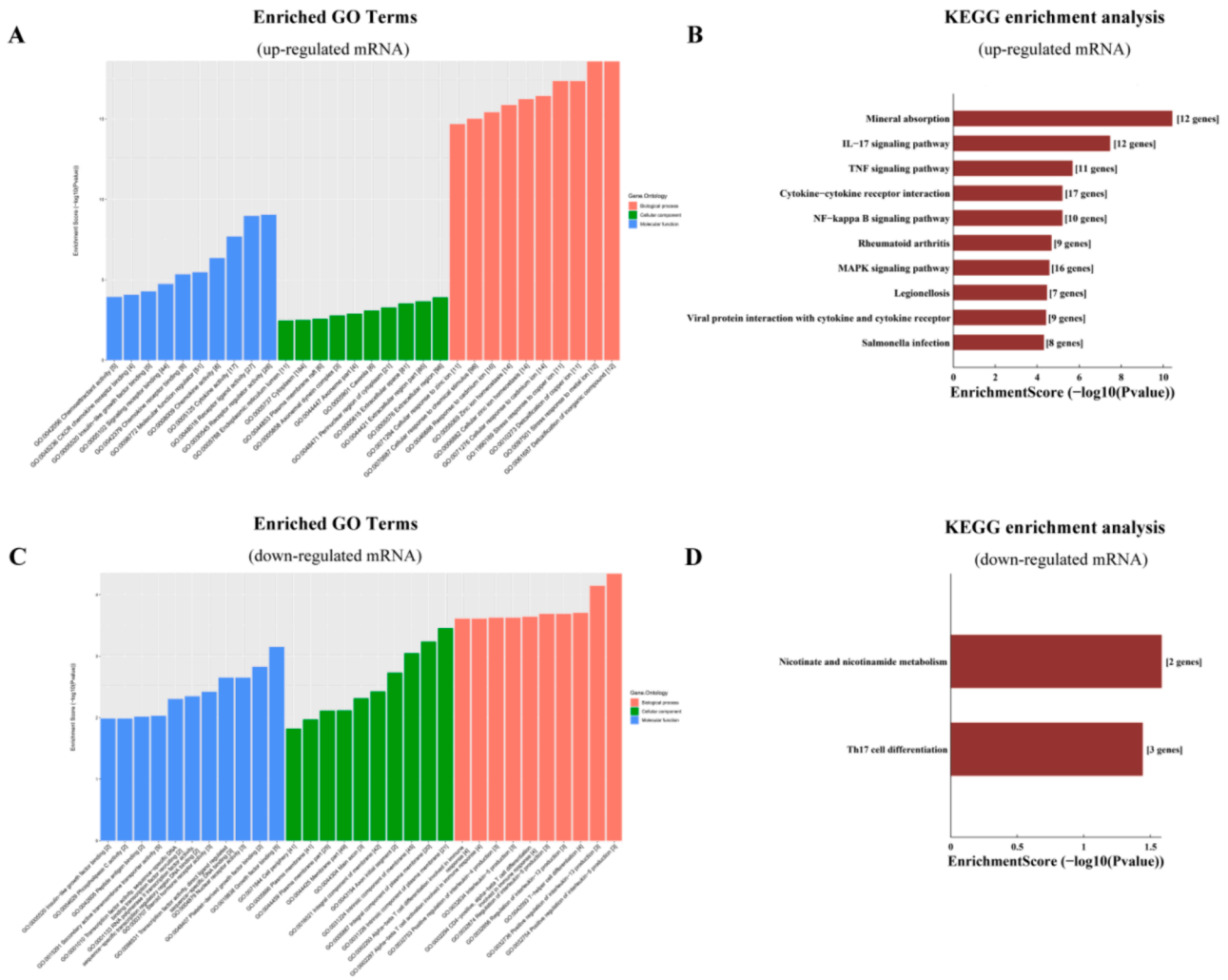

Fig. 3. GO enrichment analysis and KEGG pathway analysis of differentially expressed mRNAs. (A) GO enrichment analysis of upregulated mRNA entries bar chart; (B) Histogram of up-regulated mRNA KEGG pathway analysis; (C) Down-regulated mRNA GO enrichment analysis entry bar chart; (D) Down-regulated mRNA KEGG pathway analysis histogram.

Discussion

Several studies have demonstrated that Cd can induce the toxic effects on various types of cells. Even at low doses, prolonged exposure to Cd may lead to multiorgan toxicity. While Cd is known to markedly diminish cell viability and induce apoptosis, the degree of susceptibility and accumulation capacity varies among different cell lines due to their origin-specific characteristics. For instance, Xie demonstrated that exposure of L-02 cells to 40 μM Cd for 24 h resulted in excessive apoptosis (Xie et al., 2010), and An found that infecting L-02 cells with 40 μM Cd^{2+} for the same duration led to a decrease in cell viability of more than 80 % (An et al., 2014). In contrast, our work showed that exposure of L-02 cells to the low concentrations of $CdCl_2$ for 12 h actually enhanced cell proliferation. This finding diverges from the aforementioned studies, hinting that, akin to numerous documented toxins, Cd causes a "hormesis" response in cells to initiate repair function, compensation and a series of adaptive reactions. The discrepancies among the above studies indicate that there are differences in the sensitivity to Cd toxicity, influenced by factors such as cell generation, experimental environment, and experimental procedures despite the use of the same cell line. However, it's undeniable that the survival rate of L-02 cells is influenced by the concentration and time of Cd exposure. As the concentration increases or prolongation of the exposure time, the survival rate of L-02 exhibits a significant decreasing trend.

The findings from the differential analysis revealed dysregulated expression levels in 266 circRNAs, 223 miRNAs and 519 mRNAs, respectively which providing insights by transcriptome analysis after Cd exposure. Among the top 10 differential expressed mRNAs, MT1F, MT1X, MT1E, MT1B, and MT1L are all belong to the functional isoforms of metallothioneins 1 (MT1), proteins that are ubiquitously expressed across various human tissues. MTs are the small proteins abundant in cysteine, with their cysteine residues' sulfhydryl groups capable of binding heavy metals, thereby resisting the toxic effects of heavy metals and playing a crucial role in metal homeostasis (Coyle et al., 2002). Numerous studies have demonstrated that Cd toxicity markedly stimulates the generation of MTs, which helps to counteract the lethal effect of Cd and reduce acute toxicity to vital organs, such as liver and lungs (Klaassen et al., 2009). In accordance with the findings of our differential expression analysis results, the various subtypes of MTs were significantly upregulated in response to Cd exposure. This upregulation serves to counteract the toxic damage inflicted by Cd and safeguard the functionality of associated antioxidant enzymes.

MBD2 ranks among the top 10 mRNAs, exhibiting a significant change in expression fold along with a significant P value ($P<0.05$). Although the exact function of MBD2 remains to be elucidated, it has been observed that its expression is significantly reduced in the bronchial epithelium of mice with chronic obstructive pulmonary disease. This reduction in MBD2 leads to an enhancement in IL-6 production

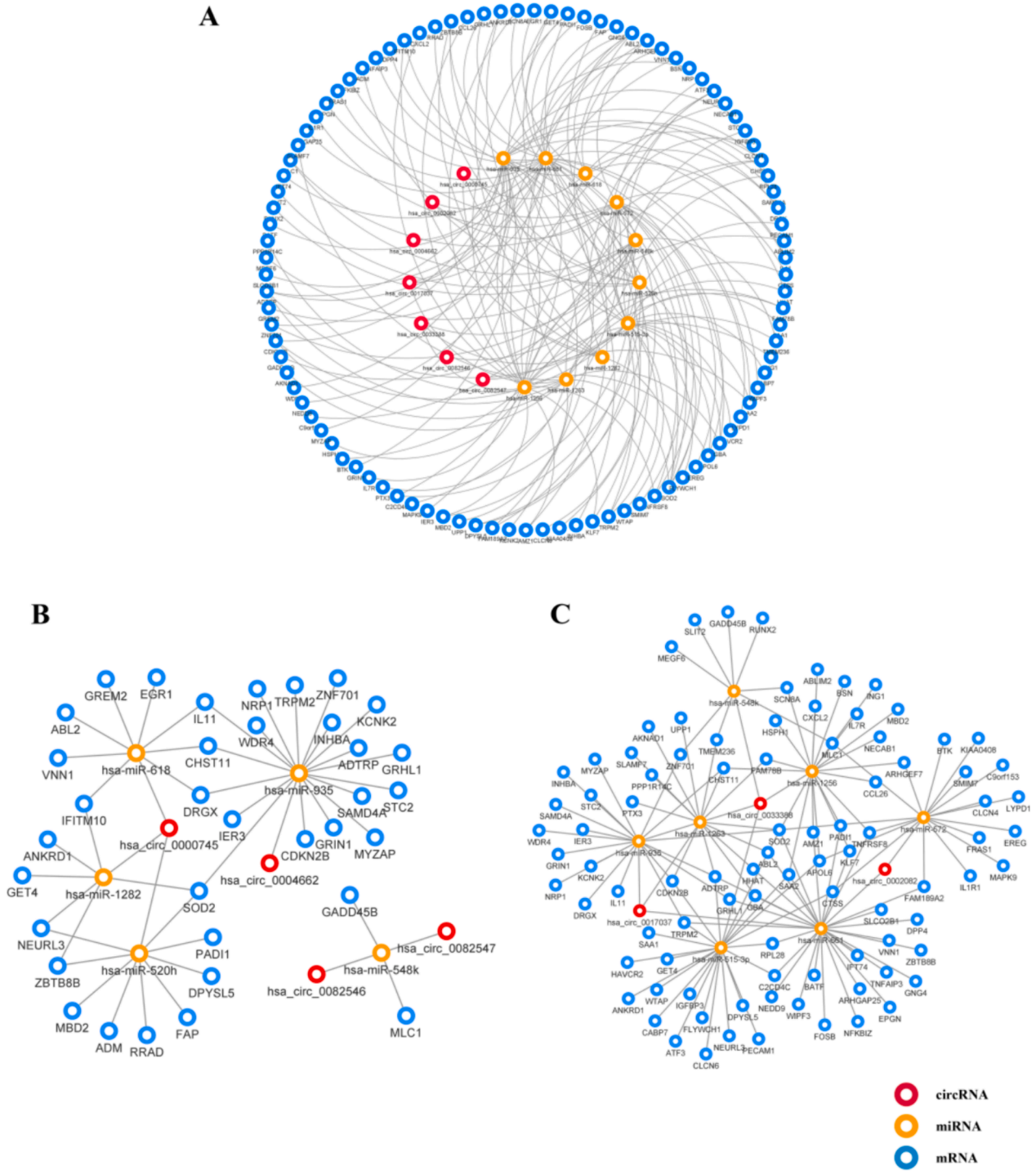

Fig. 4. Construction of circRNA-miRNA-mRNA regulatory network. (A) circRNA-miRNA-mRNA regulatory network associated with the toxic effects of Cd; (B) ceRNA pairs of hsa_circ_0004662, hsa_circ_0000745, hsa_circ_0082546 and hsa_circ_0082547; (C) ceRNA pairs of hsa_circ_0033388, hsa_circ_0002082 and hsa_circ_0017037.

through the ERK1/2 signaling pathway (Zeng et al., 2018). Moreover, a deficiency in MBD2 is shown to substantially dampen the production of transforming growth factor-β1 and reduces bleomycin-induced accumulation of M2 macrophages in the posterior lung, thereby mitigating lung injury and fibrosis (Wang et al., 2021c). Therefore, we hypothesize that MBD2 might play a pivotal role in Cd toxicity, however, further research is necessary to clarify its involvement in either promoting the inflammatory response of Cd or exerting protective effects.

Through preliminary screening and analysis of differentially expressed circRNAs, miRNAs, and mRNAs, we have identified key genes associated with the effects of Cd exposure. Specifically, the top 10 miRNAs with the most significant fold changes were found to be down-regulated, while the corresponding top 10 mRNAs were up-regulated. This finding illustrates the necessity of constructing a circRNA-miRNA-mRNA regulatory network and up-regulated circRNAs might have played the significant role.

Through GO enrichment analysis of differentially expressed mRNAs, we identified the biological processes involved in up-regulated mRNAs. These processes encompass the responses to Cd, Zn, Cu and other ions, as well as the detoxification of heavy metal ions. This suggests that the

Table 1
The main items of GO enrichment analysis of mRNA in ceRNA networks related to Cd toxicity.

GO. ID	Ontology	Term	Count	*P*-value
GO:0005615	CC	extracellular space	18	3.24E-04
GO:0005576	CC	extracellular region	18	2.35E-03
GO:0009986	CC	cell surface	9	5.70E-03
GO:0071438	CC	invadopodium membrane	2	2.96E-02
GO:0031410	CC	cytoplasmic vesicle	5	3.02E-02
GO:0031234	CC	extrinsic component of cytoplasmic side of plasma membrane	3	4.54E-02
GO:0030027	CC	lamellipodium	4	4.61E-02
GO:0000982	MF	transcription factor activity, RNA polymerase II core promoter proximal region sequence-specific binding	3	6.19E-03
GO:0002020	MF	protease binding	4	1.53E-02
GO:0001077	MF	transcriptional activator activity, RNA polymerase II core promoter proximal region sequence-specific binding	5	3.37E-02
GO:0005102	MF	receptor binding	6	3.57E-02
GO:0000978	MF	RNA polymerase II core promoter proximal region sequence-specific DNA binding	6	3.64E-02
GO:0008201	MF	heparin binding	4	4.97E-02
GO:0043065	BP	positive regulation of apoptotic process	8	7.58E-04
GO:0006954	BP	inflammatory response	8	2.88E-03
GO:0009612	BP	response to mechanical stimulus	4	3.21E-03
GO:0008285	BP	negative regulation of cell proliferation	8	3.67E-03
GO:0006357	BP	regulation of transcription from RNA polymerase II promoter	8	6.55E-03
GO:0007411	BP	axon guidance	5	8.31E-03
GO:0032715	BP	negative regulation of interleukin-6 production	3	8.59E-03
GO:0007267	BP	cell–cell signaling	6	8.92E-03
GO:0043542	BP	endothelial cell migration	3	9.20E-03
GO:0045944	BP	positive regulation of transcription from RNA polymerase II promoter	12	9.52E-03

Table 2
Information of KEGG analysis pathway of mRNA in ceRNA network.

Pathway ID	Term	Count	*P*-value
hsa04060	Cytokine-cytokine receptor interaction	7	1.95E-03
hsa04068	FoxO signaling pathway	5	6.08E-03
hsa04360	Axon guidance	4	3.24E-02
hsa04380	Osteoclast differentiation	4	3.51E-02
hsa04621	NOD-like receptor signaling pathway	3	3.80E-02

exposure of Cd lead to a variety of ion metabolism disorders. For instance, Zn, an essential trace element, can antagonize the toxic damage of Cd by stimulating the formation of MTs (Kennette et al., 2005), which help reduce ROS levels induced by Cd, thereby alleviating oxidative stress and apoptosis (Szuster-Ciesielska et al., 2000). Consequently, the passive response under the influence of Cd indicates an inherent protective mechanism. The down-regulated mRNAs were associated with several biological processes, including the positive regulation of IL-5, IL-13, and IL-4 production, T helper (TH) cell differentiation, and the regulation of IL-4 and IL-5 production, etc. It suggests that Cd toxicity affects the immune system, leading to the differentiation of Th2 cells, which subsequently promotes the secretion of IL-4, IL-5 and IL-13 (Stark et al., 2019). This not only provides insights into Cd-mediated inflammatory response but also highlights the susceptibility of exposed individuals to other diseases due to immune system abnormalities caused by Cd exposure.

KEGG pathway analysis of differentially expressed mRNAs indicated that the up-regulated mRNAs were predominantly enriched in several signaling pathways, including IL-17, TNF, NF-κB and MAPK, etc. Conversely, the down-regulated mRNAs were primarily enriched in two pathways related to nicotinate and nicotinamide metabolism, as well as Th17 cell differentiation. Epidemiological studies have demonstrated a marked increase in that the percentage of Th17 cells among lymphocyte subsets in individuals exposed to Cd (Goyal et al., 2021). Cd-induced IL-17 expression increasing in rat intestinal highlighted its pro-inflammatory impact (Ninkov et al., 2015). Consequently, Cd exposure facilitates TH cell differentiation, resulting in the production of IL-4, IL-5 and IL-13 by Th2 cells, and IL-17 by Th17 cells. This also leads to the activation of the TNF signaling pathway, culminating in the production of TNF-α. This inflammatory cascade is amplified by the activation of NF-κB and the MAPK signaling pathways, concurrently inhibiting the metabolism of nicotinate and nicotinamide (Berglund, 1994; Kim and Choi, 2015).

After conducting bioinformatics prediction, correlation test and intersection with microarray analysis, a total of 7 up-regulated circRNAs, 10 down-regulated miRNAs and 97 up-regulated mRNAs were identified and retained for further analysis. By examining the key nodes in the network, we have found that hsa_circ_0000745 targets 3 miRNAs, indicating its crucial role in the regulatory network. It has been shown to enhance the proliferation, metastasis, and glycolysis of cervical cancer cells through the regulation of the miR-409-3p/ATF1 axis, thereby serving as a miRNA sponge similar to most circRNAs (Cui et al., 2022). Likewise, up-regulation of hsa_circ_0000745 in leukemia cells promotes cell viability and inhibits cell apoptosis by activating the ERK pathway (Liu et al., 2020). Conversely, diverging from its upregulation in cervical cancer and leukemia, hsa_circ_0000745 was significantly down-regulated in gastric cancer tissues. By combining it with the receiver operator characteristic (ROC) curve originating from clinical data, it could provide good diagnostic value in clinic (Huang et al., 2017). Although there are limitations to our current knowledge of on hsa_circ_0000745, it is clear that its role in cancer is tissue-specific, manifesting in distinct expression levels and varied functionalities across different tissue types. The expression of hsa_circ_0004662 was significantly up-regulated in the inflammatory tissue of ulcerative colitis, and functional experiments demonstrated that it could decrease the trans-epithelial resistance of well-differentiated colon adenocarcinoma Caco2 cells. It suggested that hsa_circ_0004662 may mediate the disruption of the barrier function of intestinal epithelial cells, thereby contributing to the development of ulcerative colitis (Wang et al., 2019). Based on the aforementioned findings, it is hypothesized that the up-regulation of hsa_circ_0000745 may be associated with cell proliferation and apoptosis in the toxic effects of Cd. Additionally, hsa_circ_0004662 is believed to play a crucial role in the inflammatory response induced by Cd.

As a crucial component of the entire ceRNA network, miRNA is sequestered by circRNA via miRNA binding sites to modulate the function of target mRNA. In our study, utilizing the TargetScan prediction tool within the CircInteractome database, in conjunction with differential expression analysis and correlation testing, we have identified a potential interaction between hsa_circ_0000745 and hsa-miR-618, hsa-miR-1282, hsa-miR-520 h. Additionally, we have predicted a specific

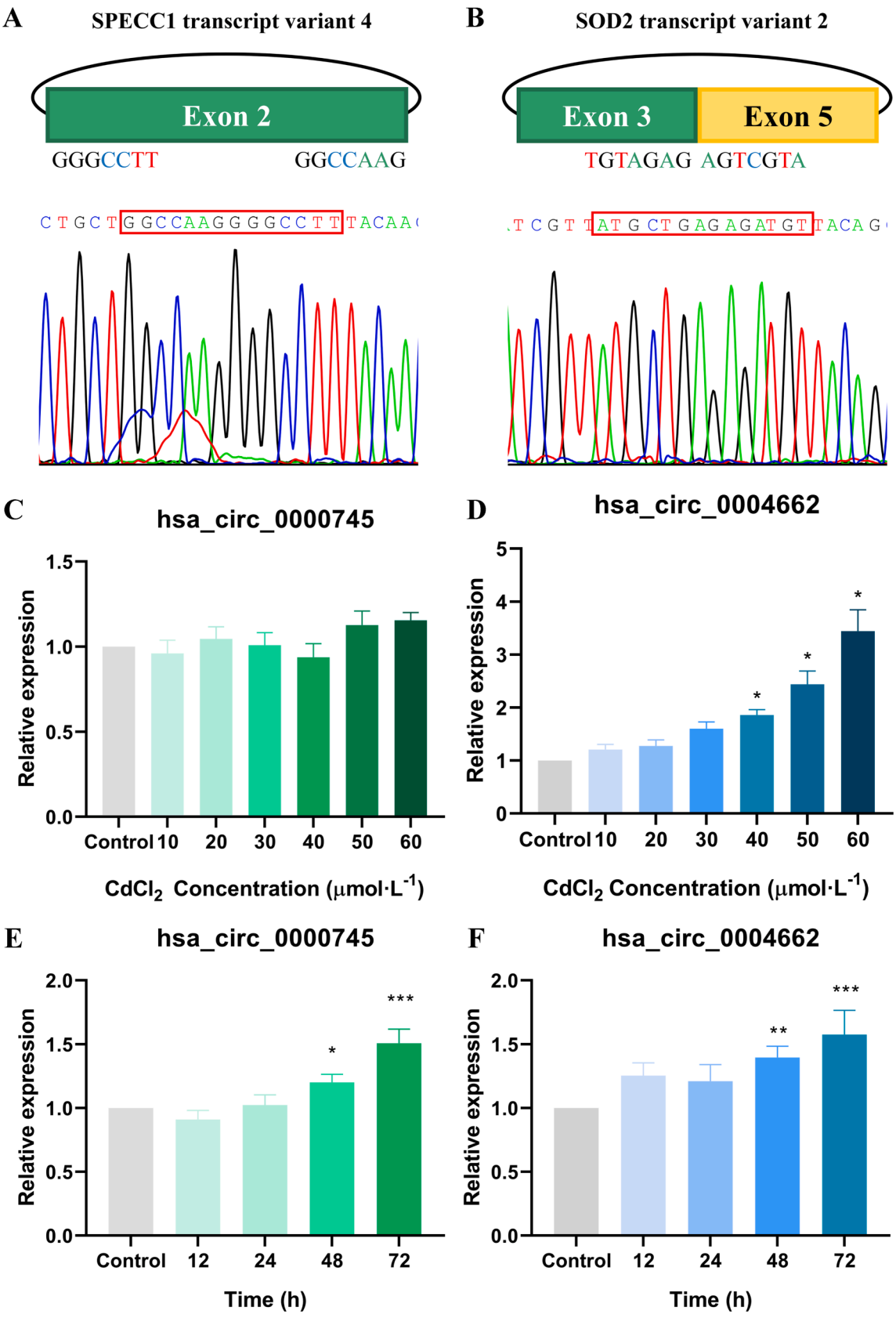

Fig. 5. Verification of circRNA expression and circular structure. (A) Hsa_circ_0004662 produced by back-splicing of exon 3 and 5 from SOD2, and transcript variant 2 as the best transcript; (B) Hsa_circ_0000745 formed through the independent circularization of exon 2 from SPECC1, and transcript variant 4 as the best transcript; (C) and (D): Effects of different concentrations of $CdCl_2$ on the expression of circ_0000745 and hsa_circ_0004662; (E) and (F): Effect of $CdCl_2$ exposure time on the expression of circ_0000745 and hsa_circ_0004662.

binding relationship between hsa_circ_0004662 and hsa-miR-935. These miRNAs have been validated to be influenced by circRNAs and play a role in various biological processes. Cao observed a negative correlation between circ-ATAD1 levels and mature miR-618 expression in colorectal cancer samples, indicating that higher circ-ATAD1 levels were associated with lower levels of mature miR-618. Based on this observation, they confirmed a direct interaction between circ-ATAD1 and the precursor form of miR-618 through RNA pull-down assays (Cao et al., 2022). The microRNA sponge activity of hsa-circ-0100153 effectively sequesters hsa-miR-935, thereby facilitating a cascade of oncogenic events central to breast cancer progression. This includes the enhancement of cellular proliferation, the facilitation of migratory capacity, the promotion of invasive potential, and the stimulation of angiogenesis, collectively contributing to the malignancy's advancement (Mokhtari et al., 2023). Our investigation has taken an initial yet significant step towards unraveling the transcriptomic alterations elicited by Cd toxicity. Through meticulous screening, we have identified pivotal circRNAs. By further predicting their associated miRNA binding sites, our findings not only enrich the current understanding of cadmium's toxicological mechanisms but also underscores the potential of circRNAs as critical mediators in Cd-induced underscores processes, offering promising leads for future therapeutic strategies and biomarker development.

Our analysis of molecular functions revealed a significant enrichment of mRNAs in transcription factor activity, transcription activator activity, protease binding, receptor binding, and heparin binding. Among these, activating transcription factors (ATFs) constitute a distinct family of transcription factors that facilitate gene expression through the recognition and binding to cyclic AMP-responsive elements. Our findings indicate that ATF3, a stress-induced transcription factor, is enriched in transcription factor activity, enabling it to respond to a multiple of signaling pathways, including endoplasmic reticulum stress, cytokines and chemokines, etc.; thereby playing a crucial role in regulating metabolism, immunity levels and tumorigenesis (Ku and Cheng, 2020). Based on the aforementioned molecular functions, it can be inferred that Cd exposure activates an array of transcription factors and transcription activators, leading to oxidative stress and cytokine-related signaling pathways. Heparin has the ability to bind to a large number of cytokines in order to regulate inflammatory damage to cells. At the biological process level, the primary enriched categories encompass the positive regulation of apoptosis, inflammatory response, negative regulation of cell proliferation, negative regulation of IL-6 production, and intercellular signaling.

KEGG pathway analysis revealed that the main enriched pathways were those involving the interaction between cytokines and cytokine receptors, specifically focusing on the FoxO and NOD-like receptor signaling pathways. FoxO proteins, a family of transcription factors, are ubiquitously expressed across nearly all tissues and control several downstream molecules involved in various biological processes, such as aging, oxidative stress, cell differentiation, apoptosis, growth and metabolism, etc. (Link, 2019). NOD-like receptors (NLRs) constitute a diverse and intricate class of signaling regulators. Some NLRs assemble into multi-protein complexes known as inflammasomes, whereas others coordinate NF-κB and MAPK signaling, stimulating inflammation responses. Chronic inflammation caused by aberrant NLR signaling can lead to chronic inflammation, genetic mutations and tumorigenesis (Saxena and Yeretssian, 2014).

The network we constructed has demonstrated its potential in predicting the functions and metabolic pathways of mRNA enrichment, which may be regulated by circRNAs. The corresponding mRNAs have the capacity to activate transcription factor activity, induce the transcription of related proteins. This activation can trigger the FoxO/NOD-like receptor signaling pathway, and the oxidation through ceRNA mechanism. Metabolic pathways associated with stress and inflammatory responses result in elevated intracellular ROS levels and extensive secretion of inflammatory factors, causing oxidative stress and inflammatory damage, which can inhibit cell proliferation and even induce to cell apoptosis.

Conclusion

Our study employed L-02 cells as a model to explore the impacts of Cadmium (Cd) exposure, revealing a pronounced dose–response and time-dependent effect. Through differential expression analysis of the whole transcriptome data related to Cd toxicity, we have identified 266 differentially expressed circRNAs, 223 miRNAs, and 519 mRNAs. Our findings highlight the capability of circRNAs to regulate their corresponding mRNAs via the ceRNA mechanism, resulting in the activation of transcription factor activity. Furthermore, it stimulates the transcription of related proteins and activates multiple pathways which are associated with stress and inflammatory responses. Consequently, there is an increase in intracellular ROS levels and the excessive secretion of inflammatory cytokines.

Notably, we have developed a novel ceRNA network that is specifically associated with seven up-regulated circRNAs under the toxic effect of Cd. This network is mainly enriched in the biological processes, including apoptosis, inflammatory response, cell proliferation inhibition, activation of the FoxO signaling pathway, and modulation of the NOD-like receptor signaling pathway. Among these, hsa_circ_0000745 and hsa_circ_0004662 have been identified as products of reverse splicing events. Our findings confirm that the differential expression of both circRNAs in response to Cd toxicity is not only significant but also suggests a pivotal role for them within the ceRNA network. This underscores their potential to influence the cellular responses to Cd exposure offering new avenues for understanding the molecular mechanisms of Cd-induced toxicity.

Credit author statement

NL conceived and designed research. ZQ, GL, CF and PW conducted experiments and analyzed data. All authors contributed with the discussion of the results. NL supervised the research. All authors read and approved this manuscript.

Declaration of competing interest

The authors declare that they have no known competing financial interests or personal relationships that could have appeared to influence the work reported in this paper.

Data availability

RNA-seq and miRNA-seq data have been submitted to the Gene Expression Omnibus (GEO accession numbers GSE246132).

Acknowledgements

The work was supported by the National Natural Science Foundation of China (81872584), Shenzhen Science and Technology Program (JSGG20220606141402005), Key R&D and Promotion Projects of Henan Province (232102310502), Natural Science Foundation of Shenzhen (JCYJ20210324093211030), Interdisciplinary Research for First-class Discipline Construction Project of Henan University (2019YLXKJC04).

RNA-seq and miRNA-seq data have been submitted to the Gene Expression Omnibus (GEO accession numbers GSE246132).

References

An, Z., Qi, Y., Huang, D., Gu, X., Tian, Y., Li, P., Li, H., Zhang, Y., 2014. EGCG inhibits Cd (2+)-induced apoptosis through scavenging ROS rather than chelating Cd(2+) in HL-7702 cells. Toxicol. Mech. Methods 24, 259–267.

Berglund, T., 1994. Nicotinamide, a missing link in the early stress response in eukaryotic cells: a hypothesis with special reference to oxidative stress in plants. FEBS Lett. 351, 145–149.
Bernhoft, R.A., 2013. Cadmium toxicity and treatment. ScientificWorldJournal 2013, 394652.
Bertin, G., Averbeck, D., 2006. Cadmium: cellular effects, modifications of biomolecules, modulation of DNA repair and genotoxic consequences (a review). Biochimie 88, 1549–1559.
Cao, L., Dong, G., Li, H., 2022. CircRNA circ-ATAD1 suppresses miR-618 maturation to participate in colorectal cancer. BMC Gastroenterol. 22, 215.
Chen, L.L., Yang, L., 2015. Regulation of circRNA biogenesis. RNA Biol. 12, 381–388.
Coyle, P., Philcox, J.C., Carey, L.C., Rofe, A.M., 2002. Metallothionein: the multipurpose protein. Cell. Mol. Life Sci. 59, 627–647.
Cui, X., Chen, J., Zheng, Y., Shen, H., 2022. Circ_0000745 promotes the progression of cervical cancer by regulating miR-409-3p/ATF1 Axis. Cancer Biother. Radiopharm. 37, 766–778.
Du, W.W., Yang, W., Liu, E., Yang, Z., Dhaliwal, P., Yang, B.B., 2016. Foxo3 circular RNA retards cell cycle progression via forming ternary complexes with p21 and CDK2. Nucleic Acids Res. 44, 2846–2858.
Goyal, T., Mitra, P., Singh, P., Ghosh, R., Sharma, S., Sharma, P., 2021. Association of microRNA expression with changes in immune markers in workers with cadmium exposure. Chemosphere 274, 129615.
Hao, R., Li, F., Song, X., Tan, X., Sun-Waterhouse, D., Li, D., 2020. Caffeic acid phenethyl ester against cadmium induced toxicity mediated by CircRNA modulates autophagy in HepG2 cells. Ecotoxicol. Environ. Saf. 197, 110610.
Huang, M., He, Y.R., Liang, L.C., Huang, Q., Zhu, Z.Q., 2017. Circular RNA hsa_circ_0000745 may serve as a diagnostic marker for gastric cancer. World J. Gastroenterol. 23, 6330–6338.
Johri, N., Jacquillet, G., Unwin, R., 2010. Heavy metal poisoning: the effects of cadmium on the kidney. Biometals 23, 783–792.
Kennette, W., Collins, O.M., Zalups, R.K., Koropatnick, J., 2005. Basal and zinc-induced metallothionein in resistance to cadmium, cisplatin, zinc, and tertbutyl hydroperoxide: studies using MT knockout and antisense-downregulated MT in mammalian cells. Toxicol. Sci. 88, 602–613.
Kim, E.K., Choi, E.J., 2015. Compromised MAPK signaling in human diseases: an update. Arch. Toxicol. 89, 867–882.
Klaassen, C.D., Liu, J., Diwan, B.A., 2009. Metallothionein protection of cadmium toxicity. Toxicol. Appl. Pharmacol. 238, 215–220.
Ku, H.C., Cheng, C.F., 2020. Master Regulator Activating Transcription Factor 3 (ATF3) in Metabolic Homeostasis and Cancer. Front Endocrinol (lausanne) 11, 556.
Kumar, S., Sharma, A., 2019. Cadmium toxicity: effects on human reproduction and fertility. Rev. Environ. Health 34, 327–338.
Link, W., 2019. Introduction to FOXO Biology. Methods Mol. Biol. 1890, 1–9.
Liu, X., Zhou, C., Li, Y., Deng, Y., Lu, W., Li, J., 2020. Upregulation of circ-0000745 in acute lymphoblastic leukemia enhanced cell proliferation by activating ERK pathway. Gene 751, 144726.
Ma, Y., Ran, D., Shi, X., Zhao, H., Liu, Z., 2021. Cadmium toxicity: A role in bone cell function and teeth development. Sci. Total Environ. 769, 144646.
Mokhtari, M., Khoshbakht, S., Esmaeil Akbari, M., Sayyed Sajjad, M., 2023. WASF3 overexpression affects the expression of circular RNA hsa-circ-0100153, which promotes breast cancer progression by sponging hsa-miR-31, hsa-miR-767-3p, and hsa-miR-935. Heliyon 9, e22874.
Ninkov, M., Popov Aleksandrov, A., Demenesku, J., Mirkov, I., Mileusnic, D., Petrovic, A., Grigorov, I., Zolotarevski, L., Tolinacki, M., Kataranovski, D., Brceski, I., Kataranovski, M., 2015. Toxicity of oral cadmium intake: Impact on gut immunity. Toxicol. Lett. 237, 89–99.
Pamudurti, N.R., Bartok, O., Jens, M., Ashwal-Fluss, R., Stottmeister, C., Ruhe, L., Hanan, M., Wyler, E., Perez-Hernandez, D., Ramberger, E., Shenzis, S., Samson, M., Dittmar, G., Landthaler, M., Chekulaeva, M., Rajewsky, N., Kadener, S., 2017. Translation of CircRNAs. Mol. Cell 66, 9–21.e27.
Panda, A.C., 2018. Circular RNAs Act as miRNA Sponges. Adv. Exp. Med. Biol. 1087, 67–79.
Sanjeev, S., Bidanchi, R.M., Murthy, M.K., Gurusubramanian, G., Roy, V.K., 2019. Influence of ferulic acid consumption in ameliorating the cadmium-induced liver and renal oxidative damage in rats. Environ. Sci. Pollut. Res. Int. 26, 20631–20653.
Saxena, M., Yeretssian, G., 2014. NOD-Like Receptors: Master Regulators of Inflammation and Cancer. Front. Immunol. 5, 327.
Stark, J.M., Tibbitt, C.A., Coquet, J.M., 2019. The metabolic requirements of Th2 cell differentiation. Front. Immunol. 10, 2318.
Szuster-Ciesielska, A., Stachura, A., Słotwińska, M., Kamińska, T., Sniezko, R., Paduch, R., Abramczyk, D., Filar, J., Kandefer-Szerszeń, M., 2000. The inhibitory effect of zinc on cadmium-induced cell apoptosis and reactive oxygen species (ROS) production in cell cultures. Toxicology 145, 159–171.
Wang, M., Chen, Z., Song, W., Hong, D., Huang, L., Li, Y., 2021a. A review on cadmium exposure in the population and intervention strategies against cadmium toxicity. Bull. Environ. Contam. Toxicol. 106, 65–74.
Wang, T.T., Han, Y., Gao, F.F., Ye, L., Zhang, Y.J., 2019. Effects of circular RNA circ-SOD2 on intestinal epithelial barrier and ulcerative colitis. Beijing Da Xue Xue Bao 51, 805–812.
Wang, Q., Pan, S., Jiang, Q., Li, L., Tu, W., Zhang, Q., Zhou, X., 2021b. CircSPAG16 suppresses cadmium-induced transformation of human bronchial epithelial cells by decoying PIP5K1α to inactivate Akt. Mol. Carcinog. 60, 582–594.
Wang, Y., Zhang, L., Wu, G.R., Zhou, Q., Yue, H., Rao, L.Z., Yuan, T., Mo, B., Wang, F.X., Chen, L.M., Sun, F., Song, J., Xiong, F., Zhang, S., Yu, Q., Yang, P., Xu, Y., Zhao, J., Zhang, H., Xiong, W., Wang, C.Y., 2021c. MBD2 serves as a viable target against pulmonary fibrosis by inhibiting macrophage M2 program. Sci. Adv. 7.
Xie, Z., Zhang, Y., Li, A., Li, P., Ji, W., Huang, D., 2010. Cd-induced apoptosis was mediated by the release of Ca2+ from intracellular Ca storage. Toxicol. Lett. 192, 115–118.
Zeng, Z., Li, M., Chen, J., Li, Q., Ning, Q., Zhao, J., Xu, Y., Xie, J., Yu, J., 2018. Reduced MBD2 expression enhances airway inflammation in bronchial epithelium in COPD. Int. J. Chron. Obstruct. Pulmon. Dis. 13, 703–715.
Zhou, X., Hao, W., Shi, H., Hou, Y., Xu, Q., 2015. Calcium homeostasis disruption - a bridge connecting cadmium-induced apoptosis, autophagy and tumorigenesis. Oncol Res Treat 38, 311–315.